Tanzania Journal of Science 47(1): 378-389, 2021
ISSN 0856-1761, e-ISSN 2507-7961

Mineralogy and Geochemistry of Shale-Hosted Copper of the Middle Buanji Group, Chimala Area, South-Western Tanzania

Almachius Mutasingwa*, Michael Msabi, Neema Jackson and Seetharamaiah Jagarlamudi
Department of Geology, The University of Dodoma, P. O. Box 11090, Dodoma, Tanzania
E-mail addresses: almach86@yahoo.com; mmsabi@yahoo.com; neemajackson205@gmail.com; jseetharamaiah@gmail.com
**Corresponding author*
Received 1 Oct 2020, Revised 9 Feb 2021, Accepted 11 Feb 2021, Published Feb 2021
https://dx.doi.org/10.4314/tjs.v47i1.32

Abstract

The mineralogical and geochemical assessments are presented in this paper to constrain the mineralogy and copper concentrations of the shale-hosted copper in the Middle Buanji Group of the Upper Paleoproterozoic (1.67 Ga). The XRD analysis revealed that illite and chamosite are the major clay minerals present in the shales together with pseudomalachite, quartz, and muscovite that constitute over 95% by proportion of the sample. The minerals biotite, birnessite, ferroselite, bearsite, chloritoid, and anatase are present in association with shale-hosted copper in low amounts (i.e., <5% by proportion of the sample). The pseudomalachite [$Cu_5(PO_4)_2(OH)_4$] is considered as ore mineral of copper in the shales of the Middle Buanji Group. Field observations revealed the presence of different shale layers within the Middle Buanji Group such as red, grey and green/blue in which copper mineral is distributed. On average, the copper concentrations in the shale layers were unevenly distributed throughout the red-grey-green shales layers with values of 0.31 wt%, 5.2 wt% and 13.19 wt%, respectively. A noticeable amount of copper mineralization up to 25.7 wt% was restricted within the green shale layer as compared to red (0.31 wt%) and grey (10.9 wt%) layers.

Keywords: Pseudomalachite; Supergene enrichment; Shale-hosted copper; Green shale layer.

Introduction

Various studies have put forward several criteria for the formation of sediment-hosted copper deposits in various geological environments such as the availability of oxidized source rocks (red beds/red shale; Oszczepalski 1999), mafic minerals and volcaniclastic materials (Brown 2006), highly reduced strata, the evaporite that acts as a hydrological seal and low-temperature brines (Brown 1997, Hitzman et al. 2010). Many of the sediment-hosted copper deposits are well reported to form in areas where continental break-up has played a significant role and subsequently lead to the formation of fault-controlled basins within 20° to 30° of the equators (Kirkham 1989, Hitzman et al. 2010) where the red beds are thin and pinched out (Selley et al. 2005). Globally, studies on the paleo plate reconstruction throughout the Earth's history have demonstrated the presence of large, economical and mineable sediment-hosted copper deposits in the Neoproterozoic to Permian basins (Volodin et al. 1994, Hitzman et al. 2010). However, the deposits that form within the late Paleoproterozoic through early Neoproterozoic contain very small sediment-hosted copper deposits (Hitzman et al. 2010) and have attracted less attention in terms of mining operations. Generally, these deposits are hosted within thin sedimentary layers with a thickness of <30 m, but the common being <3 m containing the mineable and economic copper deposits of about 1–5% (Brown 1997).

In Central African copper-bearing belts endowed with sediment-hosted copper deposits of Neoproterozoic in age have been reported in Zambia and Katanga-Congo (Cailteux et al. 2005, Hitzman et al. 2005). Copper deposits in Tanzania have received limited attention. However, Leger et al. (2018) on their explanatory notes for the Minerogenic map of Tanzania explained that the occurrence of copper deposits are associated with mafic/ultramafic, sedimentary, volcanogenic-sedimentary and metamorphic rocks from Archean to Cenozoic time. Copper has been mined in Lake Victoria, Lupa and Mpanda Gold Fields, and recovered as a by-product from the mafic/ultramafic intrusion related to massive sulfides ores, whereas in other settings, copper deposits are present in small amounts which have attracted small-scale mining operations (Schoneveld et al. 2018, Leger et al. 2018).

In the study area, the copper deposits occur in the Paleoproterozoic sediments of the Middle Buanji Group which trends in the NE-SW direction (Mbede 2002, Manya 2013). The presence of copper deposits within the Middle Buanji Group for years has been attracting the small-scale miners to participate in mining operations with hopes of getting significant income. In the study area, there is limited information on the mineralogical, geochemical assay results, exposures (outcrops) that outline the continuation of copper hosted rocks and knowledge on the nature of copper deposits. These setbacks have been affecting the small-scale miners' ability to access the deposits, thus opting random and unplanned mining operations. Therefore, the present study focused on the mineralogy and copper concentrations in the shale-hosted copper deposits within the Middle Buanji Group to constrain the distribution of copper in the shales.

Study area and geological settings

The study area is located in Mbarali district-Mbeya region and is confined within latitudes and longitudes 8° 48' 50.24" and 8° 59' 11.15" South, 34° 1' 11.24" and 34° 17' 23.86" East (Figure 1). The study area falls within the Buanji Group rocks that were mapped and described on the Quarter Sheet 246 by Harpum and Brown (1958). The area is dominated by the sedimentary rocks and lavas that overlie unconformably on the Proterozoic (2.1-1.8 Ga) (Manya 2013, Kazimoto et al. 2015) Ubendian high-grade metamorphic rocks, gabbros and granitic intrusives (Lenoir et a. 1994, Boven et al. 1999).

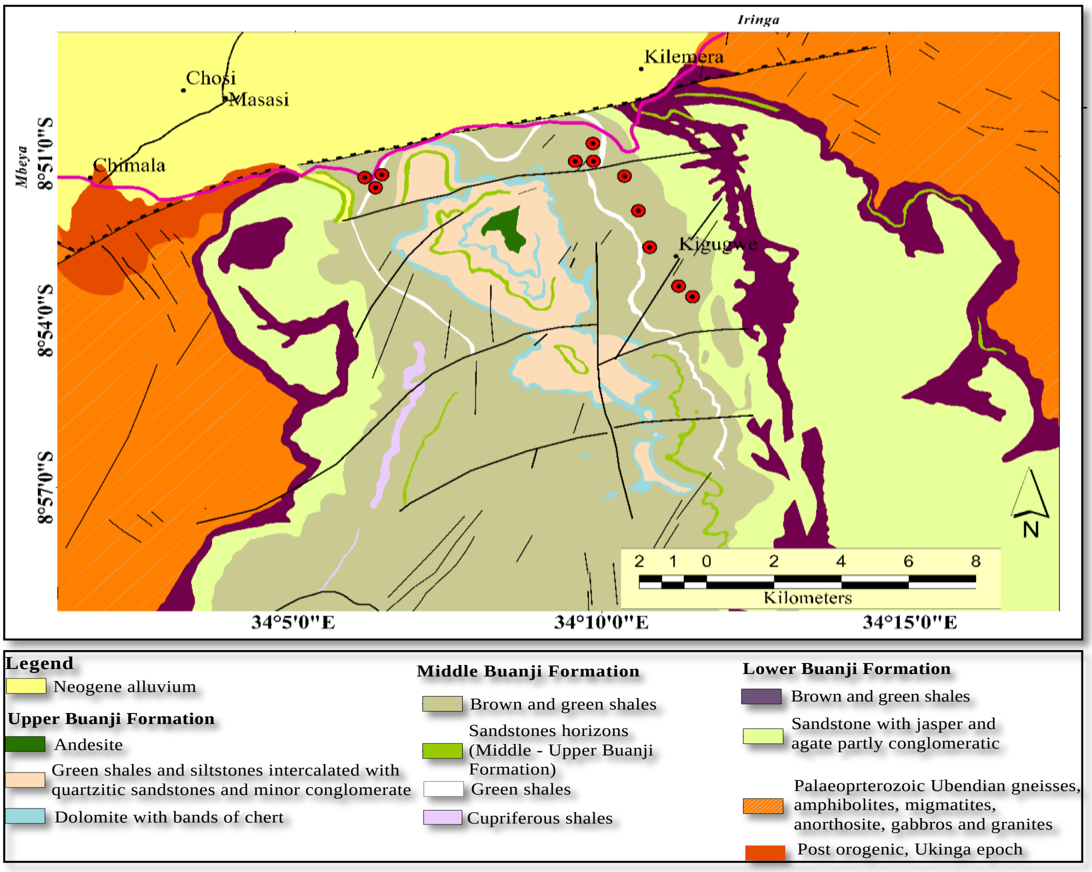

Figure 1: Map showing geology and the locations of the collected samples (solid lines indicate faults, red-spots indicates sample points) in the modified Buanji group geological map (Modified after Harpum and Brown 1958, Manya 2013 and Kasanzu et al. 2017).

Stratigraphically, the Buanji Group is subdivided into three sections (Figure 2) based on the lithological distribution which include the Lower, Middle and Upper Buanji Groups (Harpum and Brown 1958, Manya 2013) with approximate thicknesses of 245 m, 366 m and 457 m, respectively as reported by Kasanzu et al. (2017). The Lower Buanji Group contains the conglomerate which is comprised of pebbles of agate and jasper, red shales with intermittent quartzitic sandstones (Manya 2013, Kasanzu et al. 2017). The Middle Buanji Group consists of brown and green shales, dolomitic limestone, conglomerates, quartzite, sandstone and micaceous siltstone (Kasanzu et al. 2008, Manya 2013, Kasanzu et al. 2017).

The Middle Buanji shales are characterized by the cupriferous shales (Manya 2013) from which copper was constrained and locally mined by the small-scale miners. The Upper Group is characterized by greenish or greyish shales, mudstone, siltstone intercalated with sandstone and, the horizon of conglomerate and quartzite, above which they are overlaid by overlapping dolomite with chert banding. The Upper Buanji division ends with effusive volcanism represented by highly vesicular lavas on Chaufukwe Mountain (Manya 2013, Kasanzu et al. 2017). Furthermore, some of the rocks that form the Middle Buanji Group are rarely exposed due to the presence of thick soil cover in lowlands; however, at the hill-sides and tops, most of the rocks are exposed. The whole area of Buanji Group was tectonically affected by compressional deformation mechanisms that have led to various regional metamorphism and local thrusts (Harpum and Brown 1958).

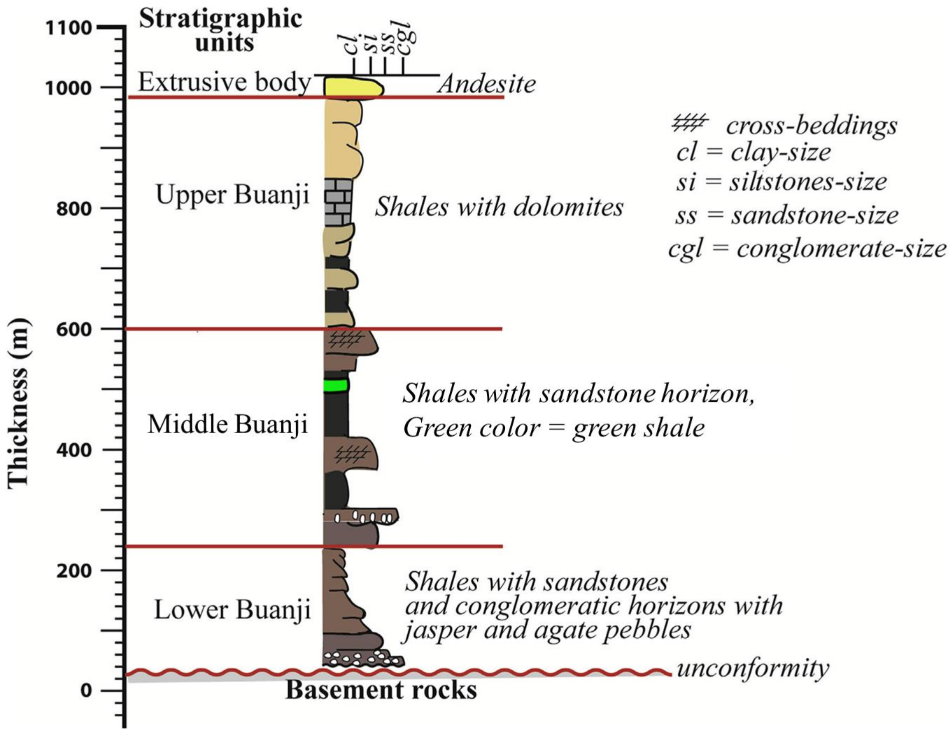

Figure 2: A stratigraphic section showing Buanji Group (Modified after Kasanzu et al. 2017).

Materials and Methods

Materials

A total of 18 rock samples were collected from the outcrop (rock exposures) and their locations are given in Figure 1. The collected samples were based on the physical properties of the shales (i.e., green and/or blue colours as an indicator of copper) both laterally and stratigraphically.

Methods

A total of 18 samples were submitted and analysed at the Geochemical Laboratory-Geological Survey of Tanzania (GST). The analyses employed the Nilton and MiniPal4 XRF pieces of equipment to determine major and trace elements concentrations in the samples. Three (3) samples out of eighteen (18) samples were analysed at the Geochemical Laboratory, Department of Geology-University of Dar es Salaam to determine the mineralogical assemblages using X-Ray Diffractometer (XRD) with model innovX InXitu Bench-BTX Top XRD, 231, cobalt (Co) X-ray tube, 30 kV acceleration voltage and 0.25 mA current. Determination of concentrations of the major and trace elements, and mineral assemblages of the samples using the XRF (X-ray fluorescence) and XRD, respectively, followed the standard procedures as illustrated in Petruk (2000).

Results

Mineralogy of the shale-hosted copper

XRD analysis of selected shale samples from the Middle Buanji Group showed the dominance of mineral assemblages in the range of silicates (quartz, muscovite, biotite, and chloritoid, ferroselite, bearsite, anatase and birnessite), non-silicate clay minerals like illite, chamosite and phosphate mineral pseudomalachite (Table 1). Only three samples out of eighteen samples were selected for XRD analysis based on their physical properties (i.e., green colour) to establish their mineral assemblages present in the shales. Green colour in shale samples was an indicative factor for the presence of copper ore minerals. Thus, the samples C_{12}, C_{14} and C_{18} showed to have most dominated with green colour compared to other shale samples.

Table 1: Mineral assemblages from the shale samples

	C_{12}	C_{14}	C_{18}
Mineral phase	**Wt %**	**Wt %**	**Wt %**
Illite	19.51	10.19	41.37
Chamosite	17.28	--	17.18
Quartz	56.43	12.83	28.95
Birnessite	4.68	--	--
Pseudomalachite	2.10	--	6.09
Muscovite	--	74.21	--
Ferroselite	--	0.47	--
Bearsite	--	0.70	--
Chloritoid	--	1.60	--
Anatase	--	--	3.67
Biotite	--	--	2.74

-- = value not detected

Major elements

The results of major elements of the Middle Buanji Group shale samples are given in Table 2. The results showed significant compositional variations, of which silica (SiO_2) ranged from 38.84 to 59.6 wt%, (average = 49.31 wt%). The shale samples also contained CuO (0.39-32.2 wt%, average = 12.26 wt%), Al_2O_3 (0.1-10 wt%, average = 8.02 wt%), Fe_2O_3 (4.23-10.4 wt%, average = 7.31 wt%), K_2O (2.19-3.04 wt%, average = 2.59 wt%), CaO (0.15-0.78 wt%, average = 0.34 wt%) and ZrO_2 (0.14-0.26 wt%, average = 0.19 wt%). The conversion of CuO to elemental composition (Cu metal) shows the variation of copper concentrations among red shales (0.31 wt%), grey shales (0.35-10.9 wt%, average = 5.2 wt%) and green shales (0.31-25.7 wt%, average = 13.17 wt%). The trace element composition of the analysed shale samples displayed wide variations in terms of concentrations, such as Mn 290-19600 ppm, Ti 3560-4680 ppm, P 3700-4610 ppm, Ba 130-7730 ppm and S 10-3050 ppm (Table 2).

Table 2: Major elements (wt%) and trace elements (ppm) compositions of Middle Buanji group shales

Sampled shale layers	**Red shale layer**	**Grey shale layer**						**Green shale layer**											
Sample Id	**C_1**	**C_2**	**C_8**	**C_{10}**	**C_{12}**	**C_{15}**	**C_{16}**	**C_3**	**C_4**	**C_5**	**C_6**	**C_7**	**C_9**	**C_{11}**	C_{13}	**C_{14}**	**C_{17}**	**C_{18}**
Concentration (wt%)																		
SiO_2	52.4	38.84	54.3	47.4	59.6	43.6	51.9	51.3	47.4	51.2	44.4	52	46.8	52.1	52	44.2	45.9	52.4
Al_2O_3	9.5	8.1	9.8	7.8	0.1	9.5	7.8	10	8.8	9.5	6.8	9	7.6	7.9	7.7	7.4	8.7	8.4
Fe_2O_3	7.48	10.4	5.83	8.59	4.23	9.51	8.89	6.09	8.91	4.34	6.59	6.48	8.93	4.61	10	4.75	6.48	9.49
CaO	0.33	0.21	0.3	0.37	0.5	0.33	0.15	0.17	0.29	0.16	0.51	0.31	0.3	0.39	0.78	0.43	0.3	0.27
K_2O	3.04	2.22	3.01	2.42	2.48	2.19	2.76	2.89	2.81	2.49	2.3	2.85	2.37	2.31	2.59	2.28	2.83	2.72
ZrO_2	0.19	0.18	0.22	0.21	0.22	0.18	0.26	0.17	0.16	0.2	0.14	0.2	0.2	0.19	0.19	0.17	0.18	0.19
CuO	0.39	10.63	1.7	2.7	13.6	9.9	0.44	17.9	2.12	26.6	28	8.5	10	32.2	32.2	12.8	0.39	10.6
Cu	0.31	8.49	1.39	2.16	10.9	7.9	0.35	14.3	1.69	21.3	22.4	6.79	8	25.7	25.7	10.2	0.31	8.49
Concentration (ppm)																		
Ti	4400	4010	3830	4110	3620	4140	4140	4680	4230	3780	3560	3980	4180	3720	4060	3630	3770	4240
Mn	290	19600	2870	2650	3470	2220	1520	460	1460	710	2030	2440	1450	940	2640	1580	2220	530
S	10	10	10	190	490	280	670	200	1970	1110	2350	3050	10	230	1050	1420	2200	10
P	4090	4270	4130	3960	4420	4290	3740	4610	3970	4430	3830	3900	4390	3700	4560	4120	4040	4050
Ba	510	1310	640	7000	190	230	150	1830	2520	1880	7730	510	740	130	210	170	210	400

Discussion

Mineralogy

The results of bulk mineralogy showed that the illite and chamosite are clay minerals present in the shales (Table 1). Neither kaolinite nor smectite was found in the shales. The other dominant non-clay minerals are quartz that ranged between 12.83 and 56.43 wt%, (average = 23.69 wt%) (Table 1), bearsite and ferroselite have displayed lower concentrations that ranged between 0.47 and 0.7 wt%. Dayal and Mani (2017) reported that illite commonly occurs in the shales controlled by the condition of weathering and high relief. Chamosite (chlorite-group minerals) occur as authigenic materials and form during the process of diagenesis in the shallow-marine environment (Ryan and Hillier 2002). The presence of mineral illite and chamosite (chlorite-group minerals) is an indication of older age formation and occur in restricted shallow marine environments in warm bottom water (>20 °C) as an ideal formation condition for these clay minerals (Net et al. 2002). The presence of chamosite in the Middle Buanji Group probably indicates a shallow-marine environment in which shales were deposited. The pseudomalachite [$Cu_5(PO_4)_2(OH)_4$] is the phosphate copper-bearing mineral associated with other silicate minerals like muscovite, birnessite, anatase and biotite.

Major elements

The results of the concentrations of analysed major elements are presented in Table 2, and the correlations of the elements of the shales are shown in Table 3. The oxides of potassium (K_2O) and zirconium (ZrO_2) were observed to be the most abundant in the shale samples because of their high positive correlations (i.e., r = 0.53 and 0.54, respectively) with SiO_2 (Table 3). The Ti, V, As, Cr, Ba and Nb were observed from the shale-hosted copper as trace elements. The copper is positively correlated with calcium and barium elements, but weakly correlated with phosphorus.

Copper concentrations and distribution

Hitzman et al. (2010) reported that sediment-hosted copper deposits formation is considered to form in geological environments characterized by the fault-controlled basins in which copper-bearing fluids migrated and precipitated in the overlying strata. Several fault sequences have been identified in the study area (Figure 1) which probably indicates the major conduit structures resulting in migration of the copper-rich fluids from its sources to the overlying strata and surrounding lithologies. A similar observation has been reported in sedimentary rock-hosted stratiform copper deposits through Earth's history in Australia (Hitzman et al. 2010). Basin characteristics are among the important factors in controlling the escape, migration and precipitation of copper-rich metal into geological formations. This has also been reported elsewhere, that precipitated copper-rich fluids are found in association with overlying marine or lacustrine shales, sandstone and carbonates (Jowett 1986, Brown 1992, Hitzman et al. 2010).

Table 3: Correlation matrix of the major and trace elements in shales from Middle Buanji Group

	SiO_2	Al_2O_3	Fe_2O_3	CaO	K_2O	ZrO_2	CuO	Ti	Mn	S	P	V	Zn	Sr	As	Cr	Ba	Nb
SiO_2	1.00	-0.34	-0.43	0.13	0.53	0.54	0.07	-0.02	-0.51	-0.06	0.09	-0.22	-0.49	0.00	-0.24	-0.26	-0.10	-0.52
Al_2O_3		1.00	0	-0.44	0.33	-0.20	-0.15	0.45	-0.10	-0.03	-0.09	0.24	-0.03	-0.03	-0.05	0.18	-0.36	-0.05
Fe_2O_3			1.00	0.01	-0.06	0.00	-0.27	0.56	0.36	-0.18	0.04	0.25	0.09	0.25	-0.24	0.68	-0.08	0.56
CaO				1.00	-0.25	-0.22	0.47	-0.39	-0.10	0.23	0.13	-0.21	-0.29	0.23	-0.21	0.11	0.51	-0.09
K_2O					1.00	0.24	-0.47	0.33	-0.35	0.00	-0.05	0.08	-0.57	0.06	-0.04	0.19	-0.35	-0.13
ZrO_2						1.00	-0.34	0.04	0.00	-0.31	-0.09	-0.17	-0.15	-0.23	-0.38	-0.31	-0.48	-0.11
CuO							1.00	-0.25	-0.06	0.21	0.23	-0.06	0.16	0.24	0.15	-0.04	0.56	-0.34
Ti								1.00	-0.08	-0.26	0.31	0.46	0.18	0.26	0.09	0.52	-0.31	0.18
Mn									1.00	-0.15	0.13	0.49	0.24	0.16	0.45	0.36	-0.01	0.86
S										1.00	-0.28	-0.37	0.00	0.26	0.21	-0.18	0.45	-0.14
P											1.00	0.65	0.10	0.38	0.15	0.28	0.05	0.15
V												1.00	0.07	0.10	0.50	0.42	-0.10	0.58
Zn													1.00	0.09	0.32	0.05	0.32	0.17
Sr														1.00	0.12	0.51	0.34	0.12
As															1.00	0.19	0.20	0.42
Cr																1.00	0.17	0.53
Ba																	1.00	-0.03
Nb																		1.00

The copper concentrations within the Middle Buanji Group are dominated within the green shale layer ranging between 0.31-25.7 wt%, average = 13.19 wt%; whereas the concentrations of 0.35-10.9 wt%, average = 5.2 wt% and 0.31 wt% were found in the grey and red shale layers, respectively. The enrichment process is supported by the observed copper concentrations (Table 2) that increase from red, grey and to green shale layers (Figure 4). This indicates that copper has been leached from the sediments (probably from the red shales and surrounding rocks), infiltrated and accumulated further downward in the green shales. This is well observed in Figure 4 where copper concentrations increase from 0.31 wt%, 8.49 wt% and 14.3 wt% Cu in red, dark and green shales, respectively. This is well described in Figure 3 A and B from which the colour of shales changed from the red, grey to green/blue relative to the increase of copper concentrations. This indicates that green shales in the sedimentary succession within the Middle Buanji Group are the major copper hosting, characterized by fine-grained and disseminated copper mineralization (Figure 3 C and D).

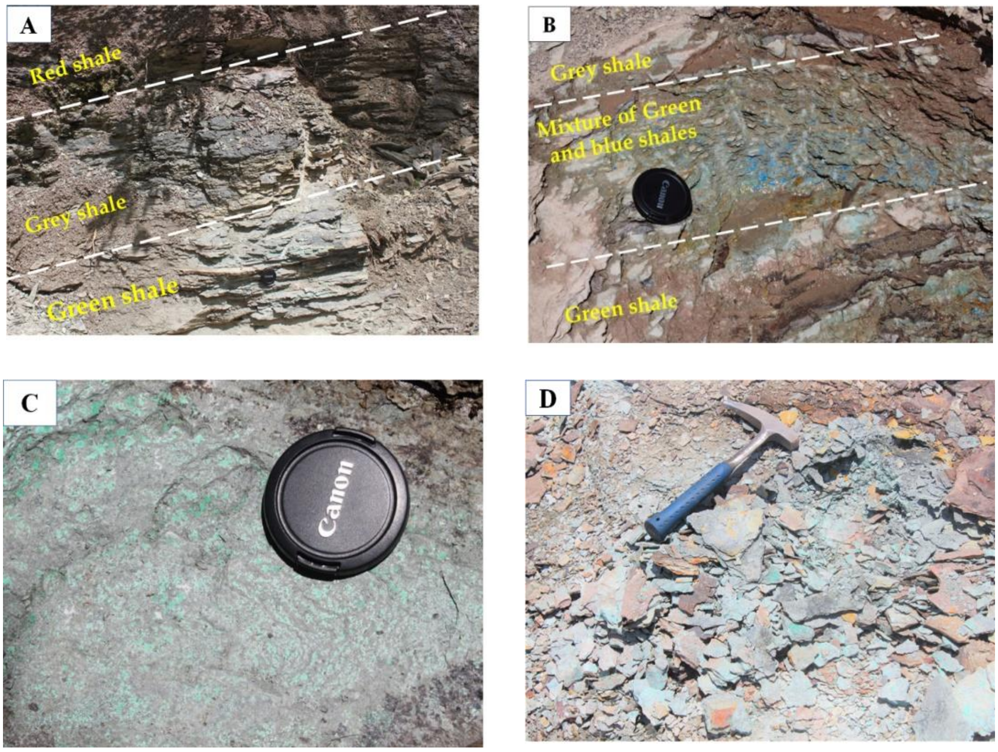

Figure 3: A and B - Shale layers with variable colours from the red to the green shale. C and D - disseminated fine-grained copper minerals in the shales.

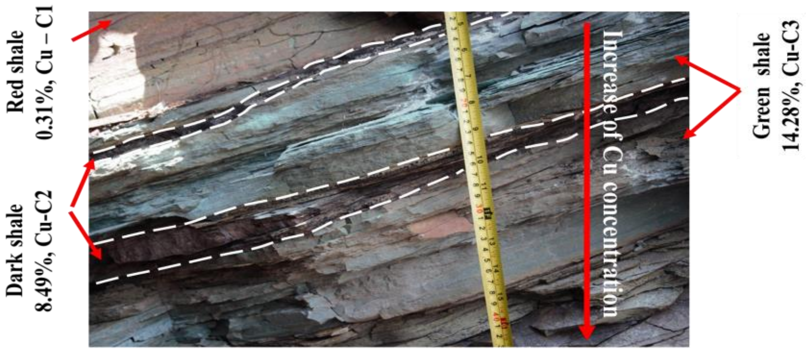

Figure 4: Down-ward increase of copper concentration throughout the shale layer succession (C1, C2 and C3 are sample numbers with their respective copper concentrations from Table 2).

The geochemical results showed variable sulfur concentrations that ranged between 10 ppm (red shale), 10–670 ppm (grey shale) and 10–3050 ppm green shale. The low sulphur concentrations in the shales indicate lower mobilization and more suppressed oxidation conditions prevailed during the deposition. Similar depositional conditions were reported by Mukherjee et al. (2020) in the Bihaigarh shales in India. Thus, sulfur has a direct effect on the increase of copper concentrations between shale layers, i.e., from red to green shales. Therefore, the presence of variable sulfur concentrations in the Middle Buanji shales indicates that sulfur might have acted as the reductant material through which copper metals were able to precipitate out of their solutions into the shales. Other studies reported that the presence of reductant materials, for example, insitu organic matter or hydrocarbons in the rocks form the chemical trap that facilitates the copper-bearing fluids to precipitate (Brown 1992, Brown 1997, Hitzman et al. 2005, Hitzman et al. 2010).

Phosphate-bearing copper mineral (pseudomalachite)

Phosphorus-bearing mineral apatite has been reported to be among the most common minerals that constitute the Earth's crust as primary and secondary grains in shales, limestone and coal (Donelick et al. 2005). Geochemical analysis of shale samples in the study has reported the presence of phosphorus concentrations between 3740 and 4560 ppm (Table 2). This indicates that phosphorous might have been sourced from the phosphate-bearing minerals apatite and become equilibrated with shales. This has also been revealed through XRD analysis of the Middle Buanji Group shales (Table 1). Crane et al. (2001) and Hewawasam (2013) reported that the aqueous solutions that infiltrate into a deeper depths leach and replace malachite [$Cu_3(OH)_2(CO_3)$] to form pseudomalachite [$Cu_5(PO_4)_2(OH)_4$]. It is suggested that phosphate ions are considered to have contributed to replacing the carbonate ions from the copper-rich carbonates (malachite) to form pseudomalachite mineral. Thus, the increase of copper concentrations downward into the green shale (Figure 4) is tied with continuous leaching, replacement of CO_3^{2-} ions by PO_4^{3-} ions resulting to downward percolation and concentration of pseudomalachite mineral. This is in agreement with the supergene enrichment process controlling the formation of pseudomalachite (El Desouky et al. 2010, Hewawasam 2013). Therefore, it can be highlighted that the supergene enrichment process is the possible formation of the phosphate copper-bearing mineral (pseudomalachite) within the shales of the Middle Buanji Group.

Conclusion

Mineralogy and geochemistry study of the Middle Buanji shales have revealed the following: (1) The most dominant minerals in the shale-hosted copper of the Middle Buanji Group include clay minerals illite and chamosite which indicate the shallow-marine depositional environment and non-clay minerals; pseudomalachite (phosphate-bearing copper mineral), muscovite, quartz and anatase. (2) The copper concentrations were unevenly distributed throughout the shale layers (i.e., red, grey and green) within the Middle Buanji Group. The green shale layers are dominated with the copper concentrations ranging from 0.31 to 25.7 wt%, average = 13.19 wt%, whereas grey and red shale layers contained 0.35-10.9 wt%, average = 5.2 wt% and 0.31 wt%, respectively. Furthermore, the study has investigated the presence of disseminated copper mineralization within fine-grained green shale in the Middle Buanji Group. The mineralization has been revealed to occur within the phosphate-bearing mineral pseudomalachite referred to as an ore mineral.

Acknowledgement

We acknowledge the financial assistance we received from the University of Dodoma under the Junior Academic Staff Funding Programme. The Geological Survey of Tanzania (GST) and the University of Dar es Salaam Geochemistry Laboratories are acknowledged for analysing the samples.

References

Boven A, Theunissen K, Sklyarov E, Klerkx J, Melnikov A, Mruma A and Punzalan L 1999 Timing of exhumation of a high-pressure mafic granulite terrane of the Paleoproterozoic Ubende belt (West Tanzania). *Precambrian Res*. 93: 119-137.

Brown AC 1992 Sediment-hosted stratiform copper deposits. *Geosci. Can.* 19: 125-141.

Brown AC 1997 World-class sediment-hosted stratiform copper deposits: Characteristics, genetic concepts and metallotects. *Australian J. Earth Sci.* 44(3): 317-328.

Brown AC 2006 Close linkage of copper (and uranium) transport to diagenetic reddening of "upstream" basin sediments for sediment-hosted stratiform copper (and roll-type uranium) mineralization. *J. Geochem. Explor*. 89: 23-26.

Cailteux JLH, Kampunzu A, Lerouge C, Kaputo A and Milesi J 2005 Genesis of sediment-hosted stratiform copper-cobalt deposits, Central African Copperbelt. *J Afr. Earth Sci*. 42(9): 134-158.

Crane MJ, Sharpe AL and Williams PA 2001 Formation of chrysocolla and secondary copper phosphates in the highly weathered supergene zones of some Australian deposits. *Rec. Aust. Mus.* 53: 49-56.

Dayal AM and Mani D (Eds) 2017 Shale Gas: Exploration and Environmental and Economic Impacts. 1st ed, Elsevier, Amsterdam.

Donelick RA, O'Sullivan PB and Ketcham RA 2005 Apatite fission-track analysis. *Rev. Mineral. Geochem*. 58: 49-94.

El Desouky HA, Muchez P, Boyce AJ, Schneider J, Cailteux JL, Dewaele S and von Quadt A 2010 Genesis of sediment-hosted stratiform copper–cobalt mineralization at Luiswishi and Kamoto, Katanga Copperbelt (Democratic Republic of Congo). *Miner. Depos.* 45(8): 35-763.

Harpum J and Brown P 1958 Geology of Chimala. Quarter Degree Sheet 246. *Geological Survey of Tanganyika*.

Hewawasam T 2013 Tropical weathering of apatite-bearing rocks of Sri Lanka: Major element behaviour and mineralogical changes. *J. Geol. Soc. Sri Lanka* 15: 31-46.

Hitzman M, Kirkham R, Broughton D, Thorson J and Selley D 2005 The sediment-hosted stratiform copper ore system. *Economic Geol*. 100.

Hitzman MW, Selley D and Bull S 2010 Formation of sedimentary rock-hosted stratiform copper deposits through Earth history. *Economic Geol.* 105(3): 627-639.

Jowett EC 1986 Genesis of Kupferschiefer Cu-Ag deposits by convective flow of Rotliegende brines during Triassic rifting.

Economic Geol. 81: 1823-1837.

Kasanzu CH, Maboko MAH and Manya S 2017 Geochemistry and Sm-Nd systematics of the 1.67 Ga Buanji Group of southwestern Tanzania: Paleo-weathering, provenance and paleo-tectonic setting implications. *Geosci. Front.* 8: 1025-1037.

Kasanzu C, Maboko MAH and Manya S 2008 Geochemistry of fine-grained clastic sedimentary rocks of the Neoproterozoic Ikorongo Group, NE Tanzania: Implications for provenance and source rock weathering. *Precambrian Res*. 164: 201-213.

Kazimoto EO, Schenk V and Appel P 2015 Granulite-facies metamorphic events in the northwestern Ubendian Belt of Tanzania: Implications for the Neoarchean to Paleoproterozoic crustal evolution. *Precambrian Res*. 256: 31-47.

Kirkham R 1989 Distribution, settings, and genesis of sediment-hosted stratiform copper deposits. *Geological Association of Canada Special Paper* 36: 3-86.

Leger C, Barth A, Falk D, Mruma A, Magigita M, Boniface N and Stanek K 2018 Explanatory notes for the minerogenic map of Tanzania. In *Geological Survey of Tanzania (GST)*.

Lenoir JL, Liégeois JP, Theunissen K and Klerkx J 1994 The Palaeoproterozoic Ubendian shear belt in Tanzania: Geochronology and structure. *J. Afr. Earth Sci*. 19(3): 169-184.

Manya S 2013 Geochemistry and U–Pb zircon dating of the high-K calc-alkaline basaltic andesitic lavas from the Buanji Group, South-Western Tanzania. *J. Afr. Earth Sci*. 86: 107-118.

Mbede E 2002 Interpretation of reflection seismic data from the Usangu, East African rift system. *Tanz. J. Sci*. 28(1): 83-97.

Mukherjee I, Deb M, Large RR, Halpin J, Meffre S, Ávila J and Belousov I 2020 Pyrite textures, trace elements and sulfur isotope chemistry of Bijaigarh Shales, Vindhyan Basin, India. *Minerals* 10(7): 588.

Net LI, Alonso MS and Limarino CO 2002 Source rock and environmental control on clay mineral associations, Lower Section of Paganzo Group (Carboniferous), Northwest Argentina. *Sediment. Geol*. 152: 183-199.

Oszczepalski S 1999 Origin of the Kupferschiefer polymetallic mineralization in Poland. *Miner. Depos.* 34: 599-613.

Petruk W 2000 Applied Mineralogy in the Mining Industry. 1st ed, Ottawa, Canada.

Ryan PC and Hillier S 2002 Berthierine/chamosite, corrensite, and discrete chlorite from evolved verdine and evaporite-associated facies in the Jurassic Sundance Formation, Wyoming. *Am. Mineralogist* 87: 1607-1615.

Schoneveld GC, Chacha M, Njau M, Jønsson J, Cerutti PO and Weng X 2018 The new face of informality in the Tanzanian mineral economy: Transforming artisanal mining through foreign investment? International Institute for Environment and Development Research Report, London, UK, 77 p.

Selley D, Broughton D, Scott R, Hitzman M, Bull S, Large R, McGoldrick PJ, Croaker M and Pollington N 2005 A new look at the geology of the Zambian Copperbelt. *Society of Economic Geologists, Inc.* 100: 965-1000.

Volodin R, Chechetkin V, Bogdanov YV, Narkelyun L and Trubachev A 1994 The Udokan cupriferous sandstone deposit (eastern Siberia). *Geol. Ore Deposits* 36(1): 1-25.